

ORIGINAL ARTICLE

Preferential PPAR- α activation reduces neuroinflammation, and blocks neurodegeneration *in vivo*

Mohammad A. Esmaili^{1,†,‡}, Shilpi Yadav^{1,†}, Ravi Kr. Gupta², Garrett R. Waggoner¹, Abigail Deloach¹, Noel Y. Calingasan³, M. Flint Beal³ and Mahmoud Kiaei^{1,*}

¹Department of Neurobiology and Developmental Sciences, Center for Translational Neuroscience and,

²Department of Microbiology and Immunology, College of Medicine, University of Arkansas for Medical Sciences, Little Rock, 72205 AR, USA and ³Feil Family Brain and Mind Research Institute, Weill Medical College of Cornell University, New York, NY 10065, USA

*To whom correspondence should be addressed. Tel: +1 5015265638; Fax: +1 5015265678; Email: mkiaei@uams.edu; kiaeim@yahoo.com

Abstract

Neuroinflammation, immune reactivity and mitochondrial abnormalities are considered as causes and/or contributors to neuronal degeneration. Peroxisome proliferator-activated receptors (PPARs) regulate both inflammatory and multiple other pathways that are implicated in neurodegeneration. In the present study, we investigated the efficacy of fenofibrate (Tricor), a pan-PPAR agonist that activates PPAR- α as well as other PPARs. We administered fenofibrate to superoxide dismutase 1 (SOD1^{G93A}) mice daily prior to any detectable phenotypes and then animal behavior, pathology and longevity were assessed. Treated animals showed a significant slowing of the progression of disease with weight loss attenuation, enhanced motor performance, delayed onset and survival extension. Histopathological analysis of the spinal cords showed that neuronal loss was significantly attenuated in fenofibrate-treated mice. Mitochondria were preserved as indicated by Cytochrome c immunostaining in the spinal cord, which maybe partly due to increased expression of the PPAR- γ co-activator 1- α . The total mRNA analysis revealed that neuroprotective and anti-inflammatory genes were elevated, while neuroinflammatory genes were down-regulated. This study demonstrates that the activation of PPAR- α action via fenofibrate leads to neuroprotection by both reducing neuroinflammation and protecting mitochondria, which leads to a significant increase in survival in SOD1^{G93A} mice. Therefore, the development of therapeutic strategies to activate PPAR- α as well as other PPARs may lead to new therapeutic agents to slow or halt the progression of amyotrophic lateral sclerosis.

Introduction

Neurodegenerative diseases, spinal cord injury, multiple sclerosis and fetal alcohol syndrome toxicity all have common pathological hallmarks, including neuroinflammation and mitochondrial dysfunction. Understanding these underlying mechanisms and how to prevent or reverse them will facilitate the disease management

and therapeutic discovery. Among the neurodegenerative diseases, amyotrophic lateral sclerosis (ALS) is a fatal neuromuscular and neurodegenerative disorder in which neuroinflammation and mitochondrial dysfunction are a common denominator. ALS largely affects the motor cortex, brainstem, spinal cord and neurons, which innervate skeletal muscles. Currently, the only FDA-approved drug for ALS is Riluzole, which prolongs life-expectancy

[†]The first two authors contributed equally.

[‡]Present address: Medicinal Plants and Drug Research Institute, Shahid Beheshti University G. C., Tehran, Iran.

Received: October 14, 2015. Revised: November 6, 2015. Accepted: November 16, 2015

© The Author 2015. Published by Oxford University Press. All rights reserved. For Permissions, please email: journals.permissions@oup.com

by 3–6 months; hence, the discovery of an effective therapeutic strategy is an urgent, unmet medical need.

In a recent study, peroxisome proliferator-activated receptor (PPAR)- α regulated hepatic autophagy in mice (1), and also induced PPAR- γ co-activator 1- α (PGC-1 α) (2). Mitochondrial dysfunction in ALS has gained ample evidence with mitochondrial DNA instability and deletion, and consistent identification of missense mutations in the CHCHD10 gene for ALS (3). Mitochondria and important cellular organelles like the endoplasmic reticulum are critical for the intracellular Ca²⁺ pool and proper cellular function, and mutations in the VAPB protein that have been linked to ALS (4) increase the importance of regulating these pathways (5).

Peroxisome proliferator-activated receptors and their utility for the treatment of neurodegenerative diseases

The PPARs are ligand-modulated transcription factors with three known isoforms: PPAR- α , PPAR- β or PPAR- δ and PPAR- γ . PPAR- α is mostly expressed in the brain, liver, heart, kidney, brown adipose tissue and skeletal muscle (6,7). PPAR β/δ is robustly expressed in the cerebellum, medulla oblongata, hypothalamus, cerebral cortex and spinal cord (8). PPAR- γ has high-expression levels in brown and white adipose tissues, brain, colon, differentiated myeloid cells and the placenta (9,10). PPARs play major roles in the regulation of gene-expression programs of metabolic pathways (11). Natural PPAR ligands are primarily unsaturated fatty acids (derivatives of linolenic acid, eicosanoids and components of oxidized LDLs); synthetic ligands include fibrates and thiazolidinediones. The binding of ligands to PPARs results in dissociation of co-repressors from the PPAR/retinoid X receptor (RXR) complex and recruitment of transcriptional co-activators, including PGC-1 α , enhancing energy metabolism and mitochondrial biogenesis. PPARs regulate multiple pathways from metabolism to immune responses (11–17). The activation of PPARs has anti-inflammatory effects that are beneficial in several mouse models of neurodegenerative diseases including ALS (18–21), tauopathy (tau) (22), Huntington's disease (HD) (23), experimental autoimmune encephalomyelitis, (24) and Parkinson's disease (PD) (25). These studies suggest that specific isoforms of PPARs and their preferential activation may have utility in treating neurodegenerative diseases. The above cited studies, and our study described in this manuscript, demonstrate that the activation of PPARs regulates an array of genes to reduce inflammation. PPAR activation also reduces oxidative stress and blocks microglial activation, as well as enhancing mitochondrial biogenesis and function. We and others showed that the activation of PPAR- γ resulted in clinical efficacy in superoxide dismutase 1 (SOD1^{G93A}) mice (20,21). The activation of PPAR- α has been shown to increase the expression of PGC-1 α and to induce autophagy by increasing the expression of transcription factor EB, a master gene for lysosomal biogenesis. We therefore examined whether fenofibrate, a pan-PPAR agonist with predominant activity at PPAR- α , can either block or slow the progression of neurodegeneration in the SOD1^{G93A} transgenic mouse model of ALS.

Results

PPAR activation improves ALS-like phenotypes and extends survival

Two cohorts of SOD1^{G93A} mice were administered fenofibrate ($n = 15$, 7 males and 8 females) at 200 mg/kg/day or vehicle ($n = 14$, 7 males and 7 females) beginning at postnatal day 40 (p40) by

intraperitoneal injection and analyzed for body weight, motor performance, pathology and survival.

Weight loss analysis

Weight changes were monitored from p60 and found SOD1^{G93A} mice begin losing weight that coincided with the age of disease onset at approximately p85–p90. The weight loss was attenuated in the fenofibrate-treated cohort (Fig. 1A). The weight difference was significant between these groups at $P < 0.01$ (t-test).

Motor performance analysis

Fenofibrate or vehicle-treated SOD1^{G93A} mice were studied for motor performance with rotarod testing twice per week. SOD1^{G93A} mice in the vehicle group showed shorter latency to fall from the rotating rod at a constant speed of 12 rpm. The constant speed paradigm is the most commonly used for ALS mice and is the best suited approach to determine the differences between treated and untreated SOD1^{G93A} mice. The accelerated paradigm is not suitable to differentiate the difference at the later stage of disease in this model. Fenofibrate-treated SOD1^{G93A} mice had a longer latency to fall off the 12 rpm rotating rod from p90 onward (Fig. 1B). The performance difference was significant between these groups at $P < 0.01$ (t-test).

Survival analysis

Generally, the average survival age in SOD1^{G93A} mice in our colony is 128 ± 5 days. In this experiment, the average survival age for the fenofibrate-treated SOD1^{G93A} mice was increased to 138 ± 5 ($n = 15$) days, while the vehicle-treated group average survival age was 127 ± 3.4 days ($n = 14$). This is an increase of 11 days (8.7%), [log-rank (Mantel–Cox) P -value < 0.0001] (Fig. 1C). The mean and median of survival ages in fenofibrate-treated group were 138 and 140 days, respectively. In dimethyl sulfoxide (DMSO)-treated control group, mean and median survival ages are 127, and 128 days, respectively (Table 1). This unpaired t-test has a P -value of < 0.0001 , which is considered extremely significant.

The overall age of the onset of ALS in fenofibrate-treated SOD1^{G93A} mice delayed from 85 to 88 days to 100 days based on the rotarod and weight data (Fig. 1A and B).

Attenuation of spinal neuronal cell loss with PPAR- α activation

Two cohorts of SOD1^{G93A} mice ($n = 6$ /cohort, equal in males and females) were treated with fenofibrate or vehicle (DMSO). Fully symptomatic disease stage mice were sacrificed at 110 days of age for spinal cord motor neuron analysis. Approximately, 50% of spinal neurons have degenerated at this stage of disease. The un-biased stereological neuronal cell count software system was used to count Nissl-stained lumbar neurons in the spinal cord sections. There was a significant attenuation of neuronal loss in the fenofibrate-treated mice relative to vehicle-treated cohort (Fig. 2).

Spinal cord gliosis is reduced by PPAR activation

Lumbar spinal cord sections from SOD1^{G93A} mice treated with fenofibrate or vehicle at P110 were stained with a marker of microglia, CD11b (cluster of differentiation molecule 11b) (Fig. 3A), and marker of astrocytes, GFAP (glial fibrillary acidic protein) (Fig. 3B). Both CD11b and GFAP immunoreactivities were diminished in fenofibrate-treated SOD1^{G93A} mice compared

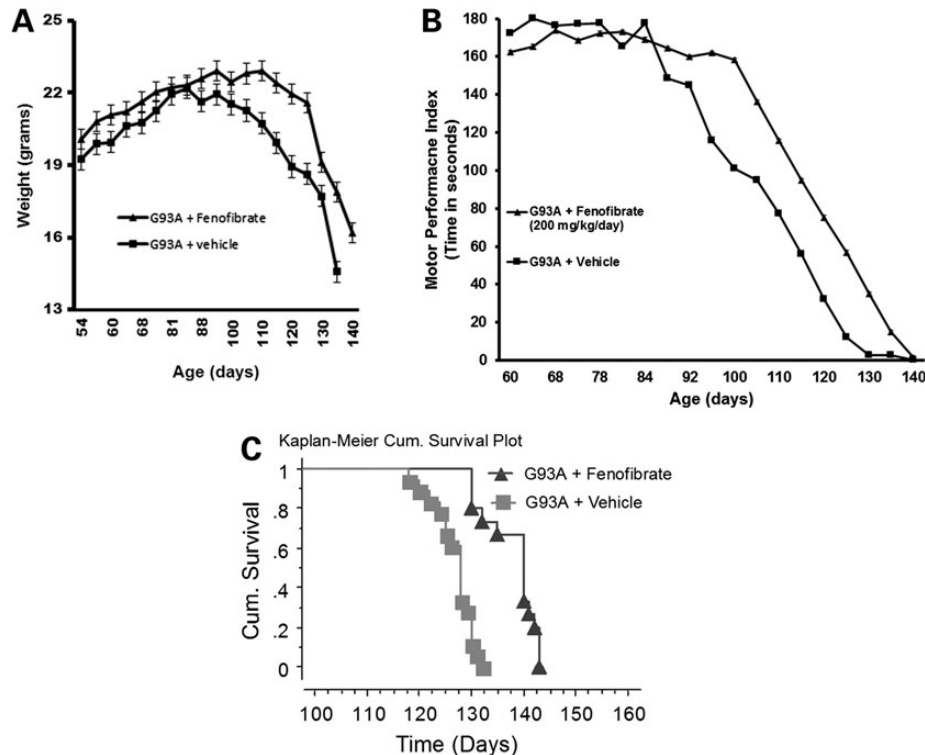


Figure 1. Fenofibrate-induced PPAR activation effects on body weight, muscle strength and survival. Body weight (A) and motor performance (B) analysis of vehicle ($n = 14$) and fenofibrate-treated mice ($n = 15$ per group). Body weight difference between treated and vehicle groups was significantly different between the ages of 105–125 days, $P < 0.01$. Motor performance using a rotarod apparatus rotating at constant speed of 12 rpm and latency to fall from the rotating rod (max 180s) was assessed and there was a significant difference observed between the ages of 95–130 days, $P < 0.01$. (C) The Kaplan–Meier survival curve of G93A mice treated with fenofibrate showing cumulative survival of fenofibrate-treated and vehicle-control mice with a statistical significant extension at $P < 0.0001$.

Table 1. Mean and median values

SOD1 ^{G93A} mice	Mean	Median (50%)
Fenofibrate treated ($n = 15$)	138	140
Control (DMSO) treated ($n = 14$)	127	128
The two-tailed P -value	< 0.0001 , extremely significant	
t -value	6.737 with 27 degree of freedom	

with untreated mice, suggesting a reduction in microglial activation and gliosis due to PPAR- α activation (Fig. 3).

PPAR activation reduces Cytochrome c release from mitochondria and increases PGC-1 α in the spinal cord

Cytochrome c and PGC-1 α are important molecules for mitochondria. Cytochrome c (a pro-apoptotic factor and a marker for trigger of apoptosis from the intrinsic pathway) if released from mitochondria will initiate apoptosis. Cytochrome c levels and release from mitochondria in the spinal cord were examined in 110-day-old SOD1^{G93A} mice treated with either fenofibrate or vehicle. The results show intense, punctate Cytochrome c immunoreactivity around the nuclei of neurons of fenofibrate-treated mice, while immunostaining was reduced in vehicle-treated SOD1^{G93A} mice (Fig. 4A). This suggests that fenofibrate blocked the release of Cytochrome c from the mitochondria of motor neurons in the spinal cord. To examine the effect of PPAR- α activation on PGC-1 α , a mitochondrial biogenesis factor,

the lumbar spinal cord sections of 110-day-old fenofibrate- or vehicle-treated SOD1^{G93A} mice were immunostained with an antibody against PGC-1 α . It was found that immunostaining was increased in the spinal cord motor neurons in fenofibrate-treated mice, when compared with vehicle-treated controls (Fig. 4B). These results show that fenofibrate up-regulates PPAR- α , blocks the release of Cytochrome c from the mitochondria and further up-regulates the expression of an array of genes to subdue multiple pathological hallmarks of ALS. Specifically, an increase in the expression of PGC-1 α , which is known to increase mitochondrial biogenesis and expression of antioxidant enzymes, was observed.

PPARs up-regulate key neuroprotective genes

To assay for elevation in neuroprotective genes under the regulation of activated PPARs, the total mRNA level isolated from spinal cords of SOD1^{G93A} mice treated with fenofibrate or vehicle ($n = 5$) were examined. Quantitative real-time polymerase chain reaction (qRT-PCR) was performed using cDNA synthesized from total RNA. PPARs (PPAR- α , PPAR- β/δ and PPAR- γ) mRNA levels were increased and PGC-1 α , nuclear respiratory factor-1, transcription factor A mitochondrial (Tfam), Sirtuin 1 (SIRT1) and Sirtuin 3 (SIRT3) were significantly increased upon fenofibrate treatment. The expression of antioxidant genes such as NAD(P)H dehydrogenase quinoneoxidoreductase-1 (NQO-1) and hemoxygenase-1 (HO-1) were restored in fenofibrate-treated mice. The mRNA for genes that produce proteins suppressor of cytokine signaling-1 (SOCS-1) and suppressor of cytokine signaling-3

(SOCS-3) were also increased several fold after fenofibrate treatment. We also checked the mRNA level of glycogen synthase kinase-3 β (GSK3 β), which is a serine/threonine protein kinase

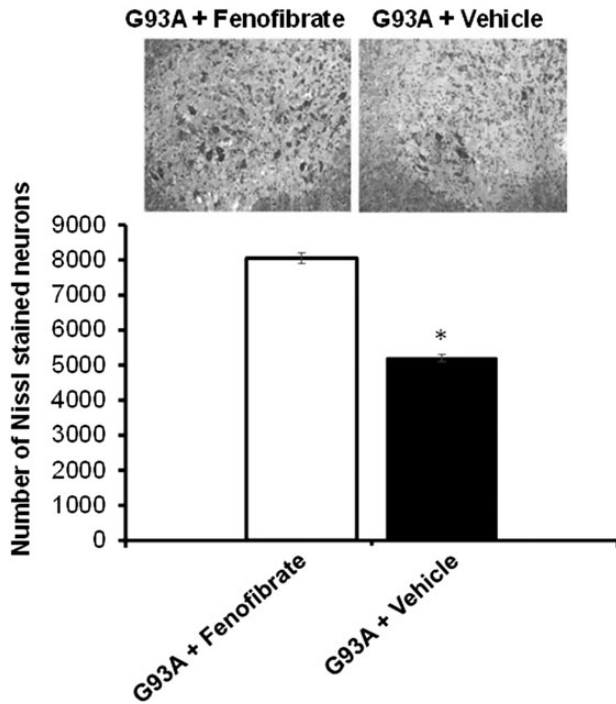


Figure 2. Fenofibrate attenuates lumbar spinal cord neuronal loss in the SOD1^{G93A} mouse model of ALS. The effect of fenofibrate treatment quantified by un-biased stereological counts of Nissl-stained neurons in SOD1^{G93A} transgenic mice. Treatment started from the pre-onset of ALS until they were sacrificed at 110 days of age. Significant attenuation of the Nissl-stained neuronal cells is evident when compared with vehicle-treated controls. * $P < 0.05$, $n = 15$, by analysis of variance and Student–Newman–Keuls tests. Values are mean \pm SD.

which is known to phosphorylate PPAR- α . No significant change was found in GSK3 β levels in the spinal cords of mice treated with fenofibrate. Although, in this study, there was no investigation of phosphorylated GSK3 β , another study with bezafibrate consistently showed no alteration in total GSK3 β (22). The activation of PPARs is known to inhibit the transcriptional regulation of many key inflammatory genes (26). The elevation of inducible nitric oxide synthase (iNOS) and cyclooxygenase-2 (COX-2) are indicative of proinflammatory responses. iNOS and COX-2 mRNA and protein levels were quantified after fenofibrate treatment (Figs 5 and 6). iNOS mRNA and protein levels were significantly reduced in fenofibrate-treated SOD1^{G93A} mice in comparison with vehicle-treated mice (Figs 5 and 6). Similarly, COX-2 mRNA and protein levels were decreased in the spinal cords of fenofibrate-treated SOD1^{G93A} mice (Figs 5 and 6). All spinal cord mRNA samples were normalized against GAPDH mRNA (Fig. 5). In protein analysis, β -actin was used as a house-keeping gene (Fig. 6).

Discussion

The list of loci, gene candidates and mutated genes linked to familial ALS (fALS) is expanding rapidly. Table 2 summarizes some of the mutations that are being most studied. TANK-binding kinase 1 (TBK1) is a gene with mutation linked to fALS and its protein mobilizes the autophagy and neuroinflammation pathways (41), interacts with optineurin (OPTN), which regulates NF- κ B, and is linked to autophagy (42). Whereas SQSTM1 is another ALS gene linked to autophagosome. Since OPTN, SQSTM1 (p62) and TBK1 function in autophagy and are linked to ALS, which they provide evidence for autophagy and neuroinflammation as important pathways in ALS due to protein/RNA aggregation.

The SOD1^{G93A} transgenic mouse, a model based on the human fALS SOD1-linked mutation, has been an effective model to study human ALS. Of all the drugs/compounds that have been tested in the SOD1^{G93A} mouse model, only Riluzole is FDA approved

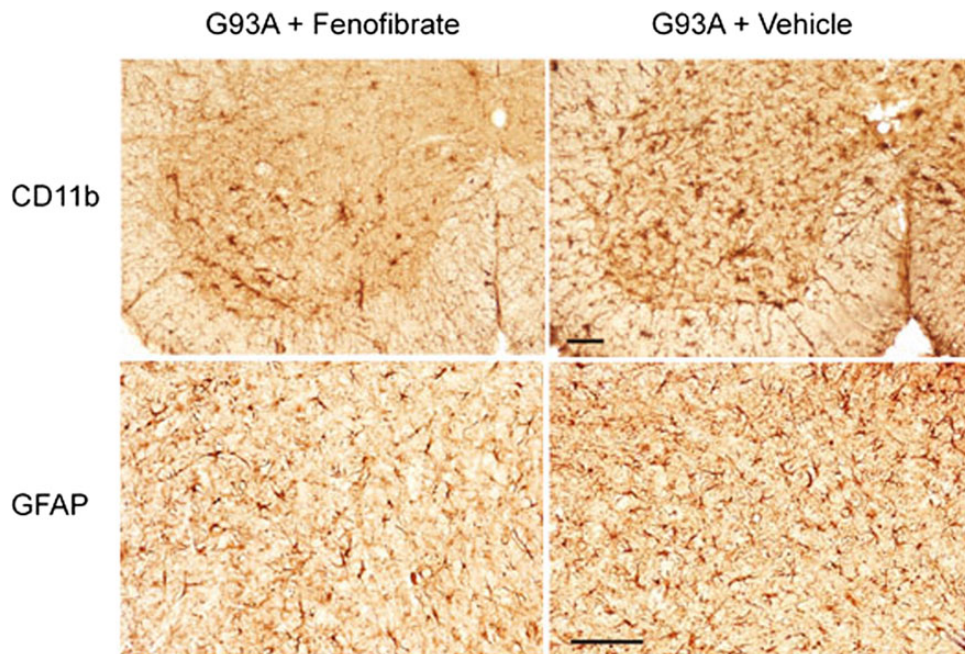


Figure 3. The effect of fenofibrate treatment on microglial activation and astrocytosis in the lumbar spinal cord of SOD1^{G93A} transgenic mice. Fenofibrate treatment reduced CD11b (marker of microglial activation) and GFAP (marker of astrocytosis) immunoreactivity in the ventral horn of the lumbar spinal cord of SOD1^{G93A} transgenic mice at 110 days of age. The scale bar is 100 microns.

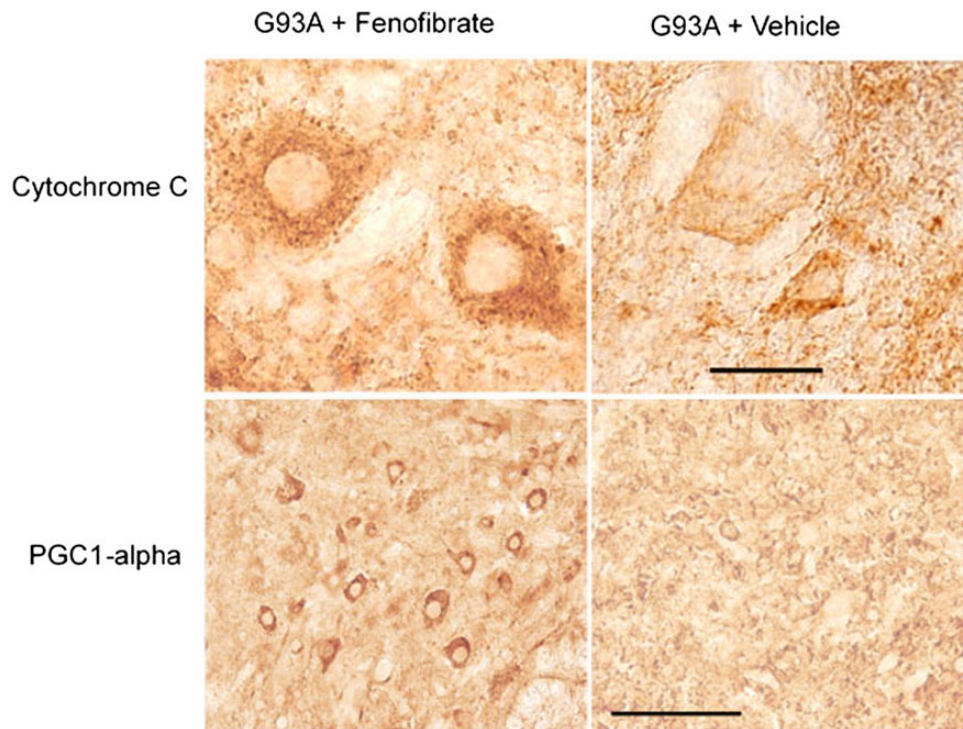


Figure 4. The effect of fenofibrate treatment on mitochondrial-related proteins in the lumbar spinal cord of SOD1^{G93A} transgenic mice. Cytochrome c (Cyto c) immunostaining is punctate (i.e. intact mitochondria concentrating around the nucleus) in fenofibrate-treated mice. Consistently, PGC1-alpha protein immunoreactivity increased in spinal cord neurons in the SOD1^{G93A} transgenic mice when compared with vehicle-treated controls. The scale bar is 100 microns.

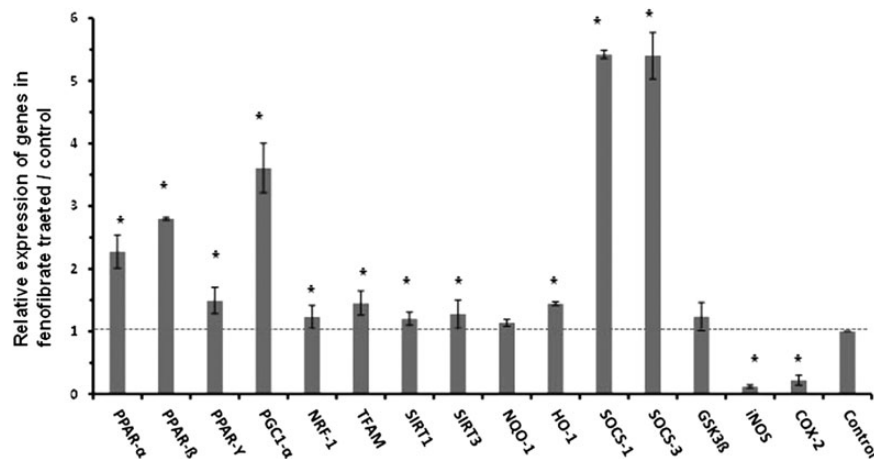


Figure 5. Fenofibrate enhances PPAR-alpha-mediated expression of PPARs: histograms shows the modulation of PPARs regulated genes, i.e. mitochondrial relevant, cytokine signaling suppressing, inflammatory, anti-inflammatory and anti-oxidative genes in the spinal cord of fenofibrate and vehicle-treated SOD1^{G93A} mice. The levels of each gene cDNA was normalized to GAPDH and expressed as fold changes relative to the vehicle-treated controls. * $P < 0.05$, $n = 5$, Student's t-test. Dotted line drawn at the height of control levels.

(reviewed in 43–45). Even though there is only modest success, the SOD1-based models are continuing to be used in testing therapeutics for ALS in conjunction with new models being developed. At this point, the testing of therapeutics is mostly limited to mouse and to some extent zebra fish models (46,47). Induced pluripotent stem cell technology, which allows the generation of human fALS motor neurons from skin fibroblasts, is an emerging model for drug testing in many neurodegenerative diseases (48).

Both of our earlier studies, as well as interesting similar findings by others on PPARs (49,50), prompted us to test the efficacy of fenofibrate, a pan PPAR activator, to further investigate the role of

the activation of PPARs in neurodegenerative diseases. Since we previously showed that PPAR- γ activation extended life span in a mouse model of motor neuron disease (20), we used the same paradigm to further test the neuroprotective effects of a pan PPAR agonist. Fenofibrate belongs to the broad fibrate class of peroxisome proliferator-receptor activators that mostly act through the α -isomer of PPAR, although it has some activity in both PPAR- γ and β/δ . It is an FDA-approved drug to treat patients with hyperlipidemia, patients with type 2 diabetes, high-cholesterol and high-triglyceride levels. In this manuscript, we present a set of new data showing neuroprotective effects of PPAR activation by

using fenofibrate, which prolongs life span in the SOD1^{G93A} transgenic mouse model of motor neuron degeneration.

Fibrates and their potential to block neurodegeneration

Fenofibrate preferentially regulates PPAR- α and is a member of the fibrate class of hypolipidemic drugs that have been extensively used to treat hypertriglyceridemia and mixed hyperlipidemia. Fenofibrate is a promising drug for ALS and perhaps other neurodegenerative diseases, because it regulates PPARs, which in turn reduces neuroinflammation and promotes mitochondrial stability. Accumulating evidence supports mitochondrial involvement, and in multiple studies we have shown mitochondrial dysfunction and decreased mitochondrial Ca²⁺ capacity (51), impaired mitochondrial dynamics and bioenergetics (52), increased production of mitochondrial reactive oxygen species and reduced mitochondrial respiration in ALS. There

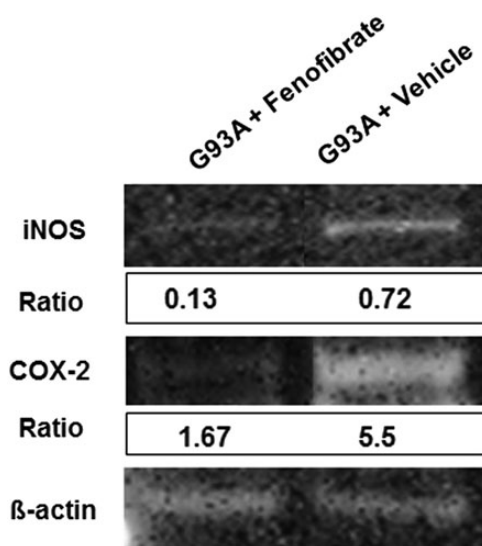


Figure 6. Fenofibrate reduces the expression of inflammatory molecules. Western blot analysis of SOD1^{G93A} control and fenofibrate-treated spinal cord homogenates (30 μ g/lane) subjected to polyacrylamide electrophoresis using iNOS, COX-2 antibodies shows significant reduction in iNOS and COX-2. Arbitrary values indicate the densitometry of bands ratios normalized against β -actin.

are key studies that convincingly implicate mitochondria as a target of mutant SOD1 toxicity, hence supporting our rationale for using fenofibrate to reduce inflammation, oxidative damage and enhancing mitochondrial function.

PPARs as targets against neurodegeneration

PPARs are known to inhibit the expression of inflammatory genes in several models.

These inflammatory genes include: nuclear factor- κ B (NF- κ B), NF of activated T cells, activator protein 1 and signal transducers and activators of transcription (53). While natural PPAR ligands are primarily unsaturated fatty acids, synthetic ligands including fibrates and thiazolidinediones are being used as drugs. Genes involved in energy metabolism, particularly lipid metabolism, adipocyte differentiation and mitochondrial biogenesis are downstream of PPARs (54–56). Certain PPAR agonists increase mitochondrial oxidative phosphorylation capacity in mouse and human cells (57,58). Sigma receptor 1 (SIGMAR1) mutations were shown to cause mitochondrial dysfunction in a cell model of ALS (59) adding evidence that implicates mitochondrial dysfunction, and providing a rationale that boosting mitochondrial function could benefit ALS patients. Fenofibrate protects against 3-nitropropionic acid, a potent mitochondrial inhibitor, 1-methyl-4-phenyl-1,2,3,6-tetrahydropyridine, a neurotoxin which cause degeneration of dopaminergic neurons in PD, stroke and traumatic brain injury (60,61). We recently showed that fibrates such as bezafibrate have robust neuroprotective effects in the R6/2 transgenic mouse model of HD. Bezafibrate increased PGC-1 α , PPARs and downstream genes, increased the number of mitochondria, improved phenotype and survival, and attenuated neuronal atrophy and astrogliosis (23). In another study using the P301S transgenic mouse model for Tau, bezafibrate treatment significantly improved behavioral deficits, reduced numbers of phospho-tau immunoreactive neurons and increased PPAR- α , PPAR- γ , PPAR- δ , Tfam, Cytochrome c, ATP synthase, hemeoxygenase-1 (HO-1) and glutathione peroxidase 1 (Gpx-1) and both full-length and N-terminal truncated PGC-1 α mRNA, showing that multiple pathways were targeted by PPAR activation (22). Another recent study showed that fenofibrate upregulates a class of proteins, cytochrome P450 4Fs (Cyp 4fs) that are involved in detoxification of the potent pro-inflammatory eicosanoid, leukotriene B₄ (LTB₄) to 20-hydroxy LTB₄ (62). Bezafibrate enhances lipid metabolism and oxidative capacity in fibroblasts or

Table 2. List of genes linked to fALS.

Genes	Cellular pathway	Disease genetic linkage	References
SOD1	Aggregation, oxidative stress, mitochondria, ER stress	ALS1	(27)
Vesicle-associated binding protein	ER stress, mitochondria	ALS	(4)
Valosin-containing protein	Mitochondria, autophagy	ALS	(28)
Amyotrophic lateral sclerosis 2		ALS2	(29)
Fused in sarcoma/translocated in liposarcoma	Aggregation, RNA metabolism	FTD/ALS	(30)
Transactive response DNA binding protein	Aggregation, RNA metabolism	FTD/ALS	(31,32)
Hexanucleotide expansion in chromosome 9 open reading frame 72	RNA foci, RNA metabolism, aggregation	FTD/ALS	(33,34)
SIGMAR1	Motor neuron excitability	ALS	(35)
OPTN	Apoptosis, inflammation	ALS, glaucoma	(36,37)
Ubiquilin 2	Protein degradation	FTD/ALS	(38)
Profilin 1	Cytoskeletal	ALS	(39)
Tubulin- α -4 A	Cytoskeletal, axonal/synaptic pathology	ALS	(40)
TBK1	NF κ -B pathway, neuroinflammation	ALS	(41)

myoblasts from patients deficient in mitochondrial complexes I, III and IV (58) and reduces the incidence of myocardial infarction in patients with the metabolic syndrome (63). The effect of fibrates on mitochondria is further supported by the study of Wenz *et al.* (64), showing that overexpressing PGC-1 α produced dramatic increases in survival and motor performance in mice with a genetic deficiency in a Cytochrome c oxidase (COX) subunit. Even more relevant to ALS, a recent study by Cleveland's group showed that overexpression of PGC-1 α in the muscle of SOD1^{G93A} mice improved the quality of life in terms of reduced ALS symptoms, although no increase in survival. They showed increases in mitochondrial biogenesis and activity, retention of muscle function, delayed muscle atrophy and significantly improved muscle endurance even at late disease stages (65). An increase in PGC-1 α activity therefore may be an attractive therapy for ALS due to its effect on muscle, which is supported by our present study showing that fenofibrate activates PGC-1 α and prevents spinal cord motor neuron death in SOD1^{G93A} mice.

Fenofibrate is considered safe, with few known side-effects. A cautionary note is that fenofibrate, a lipid disorder treating drug, may consequently reduce weight in humans; therefore, this may be a cause for concern for neurologists. There are epidemiological studies, however, that show little evidence of human weight loss with fenofibrate use. In an FDA supported online survey of over 8000 people who used fenofibrate, only 0.3% reported weight loss, which is remarkably low. In our study, the fenofibrate-treated SOD1^{G93A} mice maintained weight more successfully than the transgenic control mice. The results from wild-type (C57BL/6J) mice fed a high fat diet and given fenofibrate, which gained weight equally to a control diet (66). This study suggests that if fenofibrate causes weight loss in some patients, utilization of a high fat diet if cautiously used maybe an alternative approach to mitigate this side-effect. Two important studies regarding nutritional intake and intervention strategies and further substantiated by clinical trial that hypercaloric intake is tolerable and potentially beneficial for ALS patients (67,68). Therefore, when fenofibrate is considered for clinical testing, nutritional intake and intervention strategies should be added to the clinical trial design.

Conclusion

We demonstrate that the preferential PPAR- α activation via fenofibrate leads to neuroprotection by inhibiting neuroinflammation and protecting mitochondria in SOD1^{G93A} mice. The significant improvement in survival with fenofibrate treatment in SOD1^{G93A} mice provides evidence that it may be worthy of further development as a therapeutic strategy to block neurodegeneration in ALS.

Materials and Methods

Mouse model of ALS

Animals

All animal handling and experiments were conducted in accordance with the Institutional Animal Care and Use Committee (IACUC) guidelines of the University of Arkansas for Medical Sciences. Experiments employed hemizygous SOD1^{G93A} (69) expressing mutant human SOD1, generated on a B6SJL background strain (G93A SOD1, B6SJL-TgGur1), Jackson Laboratories, Bar Harbor, ME, USA). Our colonies of these mice were housed in UAMS animal vivarium. Wild-type females (B6SJL/F1) were purchased from Jackson Laboratories to breed with SOD1^{G93A} males. Animals were housed at room temperature in a 12 h light/dark

cycle with free access to food and water. All procedures were reviewed and approved by the IACUC of University of Arkansas for Medical Sciences prior to starting the experiments for this study.

SOD1^{G93A} mice

SOD1^{G93A} mice overexpressing human SOD1 protein with mutations on glycine to alanine at position 93. These mice develop ALS-like phenotypes from the age of 85–90 days and progressively weaken, lose weight, develop asymmetrical hind-limb tremor and paralysis, gait abnormalities, muscle atrophy, impaired motor performance, forelimb paralysis at end-stage and premature death around 128 days of age. Pathologically, the affected spinal cords exhibit extensive loss of motor neurons, marked increase in gliosis.

Fenofibrate treatment

All the treatment cohorts of SOD1^{G93A} mice were injected daily with fenofibrate (Sigma, St Louis, MO, USA) at 200 mg/kg of body weight starting at p40. Fenofibrate was dissolved in DMSO and made to 10% of the total volume injected. DMSO was used as in our previous study without any adverse effect (70).

Mouse survival and motor function

Motor ability and weight assessment

Motor performance was assessed using a rotarod apparatus (Harvard Panlab Rota-Rod apparatus, Holliston, MA, USA). This test measures the capability of mice to remain upright on the rod rotating at 12 rpm, (rotations per minute). The time elapsed before a mouse falls off the rotarod measures its competency at the task and provides a reliable indication of motor performance and progression of motor dysfunction. All mice were trained twice in a week on the rotarod and subsequently tested bi-weekly from 60 days of age. Each mouse participated in three trials per test session (max 3 min), with the best result of three trials recorded. Mice were weighed twice a week.

Survival

Mice were observed each morning. Mice were deemed to have reached end-stage of the disorder when they can no longer initiate movement after being gently agitated for 2 min or cannot right themselves when placed on their backs within 20 s. These end stage mice were euthanized by CO₂ overdose.

Histology and immunohistochemistry

Mice were deeply anesthetized with sodium pentobarbital and transcardially perfused with 4% paraformaldehyde in 0.1 M phosphate buffer, pH 7.4. Spinal cords were removed, post-fixed with 4% paraformaldehyde for 2 h, washed with 1 \times PBS (phosphate buffered saline), cryoprotected in a graded series of 10, 20 and 30% sucrose, and cut into frozen serial 35 μ m thick sections for immunohistochemical studies. Spinal cord tissue sections were stained for Nissl substance (cresyl violet) as described elsewhere (71). Avidin-biotin-peroxidase method was performed for immunohistochemistry. Briefly, free-floating 35 μ m thick spinal cord sections were treated with 3% H₂O₂ in 0.1 M PBS for 30 min. The sections were rinsed in PBS twice for 5 min each. Sections were incubated in 1% bovine serum albumin (BSA)/0.2% Triton X-100 (Sigma) for 30 min, then incubated overnight with primary antibodies (diluted in PBS/0.5% BSA) such as GFAP, (Dako, CA, USA), CD11b, PGC1- α and Cytochrome c (Santa Cruz Biotechnology, CA, USA). Biotinylated IgG secondary antibodies (diluted in PBS/0.5% BSA, Vector Laboratories, Burlingame, CA,

USA) were used for 1 h, and then incubated in avidin–biotin peroxidase complex (1:200 in PBS; Vector Laboratories) for 1 h. The immunoreaction was visualized using 3, 3'-diaminobenzidine tetrahydrochloridedihydrate (Vector Laboratories) as the chromogen. All incubations and rinses were performed at room temperature with agitation using an orbital shaker. The sections were mounted onto gelatin coated slides, dehydrated, cleared in xylene and cover slipped.

Stereological cell counts

Nissl-positive neurons were counted using standard procedures for stereological analysis as performed routinely in our laboratory as described elsewhere (71).

Western blot analysis

Expression levels of inflammatory genes such as iNOS and COX2 modulated by PPAR/RXR pathways were performed by the western blot analysis of tissue extracts from the spinal cord using standard procedures that are routinely performed in our laboratory. The β -actin was used as a house-keeping protein to normalize protein loading ($n = 3$ and representative of the replicate of three experiments presented).

RNA isolation and qRT-PCR

The total RNA was isolated from the spinal cord of fenofibrate and vehicle-treated SOD1^{G93A} mice for *in vivo* transcriptional analysis. The total RNA was isolated according to manufacturer's protocol using Trizol reagent (Invitrogen, CA, USA) and quantitated by ND-1000 NanoDrop (NanoDrop Technologies, DE, USA). The resultant 2.0 μ g of total RNA was treated with ribonuclease free deoxyribonuclease (DNase1) (Ambion, TX, USA) to remove genomic DNA contamination and checked for DNA contamination by running a no-RT-PCR using GAPDH gene primers for 25 cycles in a thermocycler. RNA was stored in -80°C until further use. One microgram of DNase-treated RNA was used to make cDNA using the iScriptc DNA synthesis kit according to the manufacturer's protocol (Bio-Rad, CA, USA). RT-PCR was performed with SYBR Green PCR Master Mix (Applied Biosystems, Foster City, CA, USA) according to the kit instructions using the ABI Prism 7300 detection system (Applied Biosystems). Briefly, 100 ng of cDNA was subjected to an RT-PCR using gene-specific primers listed in Table 1. Cycling conditions were enzyme activation at 95°C for 10 min followed by 40 cycles of denaturation at 95°C for 15 s and annealing and extension at 60°C for 1 min. Dissociation steps were at 95°C for 15 s, 60°C for 30 s (including extension) and 95°C for 15 s. Relative expression levels were determined by the comparative threshold cycle ($\Delta\Delta\text{Ct}$) method using GAPDH as a reference gene (72). Below is the list of primer sequences for genes, analyzed in this study ($n = 6$ and representative of replicate of three experiments presented).

Primer sequences for the gene expression analysis:

PPAR- α
 FWD: 5'-GTCCTCAGTGCTTCCAGAGG-3'
 REV: 5'-GGTCACCTACGAGTGGCATT-3'
 PPAR- β
 FWD: 5'-GACGGAGAGTGAGACCTTGC-3'
 REV: 5'-AACAGGAGGTGCTGAGGAGA-3'
 PPAR- γ
 FWD: 5'-CTGTGAGACCAACAGCCTGA-3'
 REV: 5'-AATGCGAGTGGTCTTCCATC-3'
 PGC1- α

FWD: 5'-TGAGAGGGCCAAGCAAAG-3'
 REV: 5'-ATAAATCACACGGCGCTCTT-3'
 NRF1
 FWD: 5'-TGGTCCAGAGAGTGCTTGTG-3'
 REV: 5'-TTCCTGGGAAGGGAGAAGAT-3'
 TFAM
 FWD: 5'-AGCCAGGTCCAGCTCACTAA-3'
 REV: 5'-AAACCCAAGAAAGCATGTGG-3'
 SIRT1
 FWD: 5'-CAGCCGTCTCTGTGTACAAA-3'
 REV: 5'-TGAAGGATCCTTTGGATTCC-3'
 SIRT3
 FWD: 5'-CTGCGGCTCTATACACAGAA-3'
 REV: 5'-CTGGAAGGACCTTCGACAG-3'
 NQO-1
 FWD: 5'-CATTCTGAAAGGCTGGTTTGA-3'
 REV: 5'-CTAGCTTTGATCTGGTTGTGAC-3'
 HO-1
 FWD: 5'-ACATCGACAGCCCCACCAAGT TCA-3'
 REV: 5'-CTGACGAAGTGACGCCATCTGTGAG-3'
 SOCS-1
 FWD: 5'-AGCAGCTCGAAAAGGCAGTC-3'
 REV: 5'-ACACTCACTTCCGCACCTTC-3'
 SOCS-3
 FWD: 5'-ACCAGCGCCACTTCTTACAG-3'
 REV: 5'-GTGGAGCATCATACTGATCC-3'
 GSK3 β
 FWD: 5'-CAACAAGGGAGCAAATTAGAGAAA-3'
 REV: 5'-TGATGCAGAAGCGGCGTTAT-3'
 iNOS
 FWD: 5'-TGGGAGCCACAGCAATATAG-3'
 REV: 5'-ACAGTTTGGTGTGGTGTAGG-3'
 COX-2
 FWD: 5'-CACAAACAGAGTGTGCGACATAC-3'
 REV: 5'-GGCAATGCGGTTCTGATACTG-3'
 GAPDH
 FWD: 5'-ATCCCAGAGCTGAACG-3'
 REV: 5'-GAAGTCCGAGGAGACA-3'

Data analysis

Estimation of sample size

Our experience with neurochemical measurements in previous animal experiments suggests that a standard deviation (SD) of 15–20% can be expected. Using the power analysis statistical program and our previous studies (73), we calculate that group sizes of 15–20 are adequate to give an 80% chance of detecting a 30% difference between groups. These results provide only estimates of sample sizes, and we predict requiring at least this number of samples to confidently exclude type II errors.

Analysis of data

Unless otherwise noted, data analysis was by analysis of variance and/or t-tests to compare sample groups, with a Bonferroni correction to correct for multiple comparisons if appropriate using the GraphPad Prism (GraphPad Software, CA, USA) InStat and Prism software. If data are not normally distributed (74), we used either the Mann–Whitney U-test or the Kruskal–Wallis test. Survival statistics were calculated from Kaplan–Meyer survival curves using the Mantel–Cox log-rank analysis. The statistical significance was at the $P < 0.05$ level.

Conflict of Interest statement. None declared.

Funding

This work was supported by grants from UAMS startup fund, UAMS Center for Translational Neurosciences, and the National Institute of General Medical Sciences IDeA award P30 GM110702.

References

- Lee, J.M., Wagner, M., Xiao, R., Kim, K.H., Feng, D., Lazar, M.A. and Moore, D.D. (2014) Nutrient-sensing nuclear receptors coordinate autophagy. *Nature*, **516**, 112–115.
- Hondares, E., Rosell, M., Diaz-Delfin, J., Olmos, Y., Monsalve, M., Iglesias, R., Villarroya, F. and Giral, M. (2011) Peroxisome proliferator-activated receptor alpha (PPARalpha) induces PPARgamma coactivator 1alpha (PGC-1alpha) gene expression and contributes to thermogenic activation of brown fat: involvement of PRDM16. *J. Biol. Chem.*, **286**, 43112–43122.
- Bannwarth, S., Ait-El-Mkadem, S., Chausse, A., Genin, E.C., Lacas-Gervais, S., Fragaki, K., Berg-Alonso, L., Kageyama, Y., Serre, V., Moore, D.G. et al. (2014) A mitochondrial origin for frontotemporal dementia and amyotrophic lateral sclerosis through CHCHD10 involvement. *Brain*, **137**, 2329–2345.
- Nishimura, A.L., Mitne-Neto, M., Silva, H.C., Richieri-Costa, A., Middleton, S., Cascio, D., Kok, F., Oliveira, J.R., Gillingwater, T., Webb, J. et al. (2004) A mutation in the vesicle-trafficking protein VAPB causes late-onset spinal muscular atrophy and amyotrophic lateral sclerosis. *Am. J. Hum. Genet.*, **75**, 822–831.
- Stoica, R., De Vos, K.J., Paillusson, S., Mueller, S., Sancho, R.M., Lau, K.F., Vizcay-Barrena, G., Lin, W.L., Xu, Y.F., Lewis, J. et al. (2014) ER-mitochondria associations are regulated by the VAPB-PTPIP51 interaction and are disrupted by ALS/FTD-associated TDP-43. *Nat. Commun.*, **5**, 3996.
- Bookout, A.L., Jeong, Y., Downes, M., Yu, R.T., Evans, R.M. and Mangelsdorf, D.J. (2006) Anatomical profiling of nuclear receptor expression reveals a hierarchical transcriptional network. *Cell*, **126**, 789–799.
- Bensinger, S.J. and Tontonoz, P. (2008) Integration of metabolism and inflammation by lipid-activated nuclear receptors. *Nature*, **454**, 470–477.
- Woods, J.W., Tanen, M., Figueroa, D.J., Biswas, C., Zycband, E., Moller, D.E., Austin, C.P. and Berger, J.P. (2003) Localization of PPARdelta in murine central nervous system: expression in oligodendrocytes and neurons. *Brain Res.*, **975**, 10–21.
- Willson, T.M., Lambert, M.H. and Kliewer, S.A. (2001) Peroxisome proliferator-activated receptor gamma and metabolic disease. *Annu. Rev. Biochem.*, **70**, 341–367.
- Sarruf, D.A., Yu, F., Nguyen, H.T., Williams, D.L., Printz, R.L., Niswender, K.D. and Schwartz, M.W. (2009) Expression of peroxisome proliferator-activated receptor-gamma in key neuronal subsets regulating glucose metabolism and energy homeostasis. *Endocrinology*, **150**, 707–712.
- O'Connor, O.A., Hamlin, P.A., Portlock, C., Moskowitz, C.H., Noy, A., Straus, D.J., Macgregor-Cortelli, B., Neylon, E., Sarasohn, D., Dumetrescu, O. et al. (2007) Pralatrexate, a novel class of antifolate with high affinity for the reduced folate carrier-type 1, produces marked complete and durable remissions in a diversity of chemotherapy refractory cases of T-cell lymphoma. *Br. J. Haematol.*, **139**, 425–428.
- Purdy, C.W., Loan, R.W., Straus, D.C., Briggs, R.E. and Frank, G.H. (2000) Conglutinin and immunoconglutinin titers in stressed calves in a feedlot. *Am. J. Vet. Res.*, **61**, 1403–1409.
- Purdy, C.W., Raleigh, R.H., Collins, J.K., Watts, J.L. and Straus, D.C. (1997) Serotyping and enzyme characterization of *Pasteurella haemolytica* and *Pasteurella multocida* isolates recovered from pneumonic lungs of stressed feeder calves. *Curr. Microbiol.*, **34**, 244–249.
- Purdy, C.W., Straus, D.C. and Ayers, J.R. (2005) Effects of aerosolized class C fly ash in weanling goats. *Am. J. Vet. Res.*, **66**, 991–995.
- O'Brien, R.J., Mammen, A.L., Blackshaw, S., Ehlers, M.D., Rothstein, J.D. and Hagan, R.L. (1997) The development of excitatory synapses in cultured spinal neurons. *J. Neurosci.*, **17**, 7339–7350.
- O'Connor, O.A., Wright, J., Moskowitz, C., Muzzy, J., MacGregor-Cortelli, B., Stubblefield, M., Straus, D., Portlock, C., Hamlin, P., Choi, E. et al. (2005) Phase II clinical experience with the novel proteasome inhibitor bortezomib in patients with indolent non-Hodgkin's lymphoma and mantle cell lymphoma. *J. Clin. Oncol.*, **23**, 676–684.
- Olasmaa, M., Guidotti, A., Costa, E., Rothstein, J.D., Goldman, M.E., Weber, R.J. and Paul, S.M. (1989) Endogenous benzodiazepines in hepatic encephalopathy. *Lancet*, **1**, 491–492.
- Portlock, C.S., Qin, J., Schaindlin, P., Roistacher, N., Myers, J., Filippa, D., Louie, D., Zelenetz, A.D., O'Brien, J.P., Moskowitz, C. et al. (2004) The NHL-15 protocol for aggressive non-Hodgkin's lymphomas: a sequential dose-dense, dose-intense regimen of doxorubicin, vincristine and high-dose cyclophosphamide. *Ann. Oncol.*, **15**, 1495–1503.
- Olasmaa, M., Rothstein, J.D., Guidotti, A., Weber, R.J., Paul, S.M., Spector, S., Zeneroli, M.L., Baraldi, M. and Costa, E. (1990) Endogenous benzodiazepine receptor ligands in human and animal hepatic encephalopathy. *J. Neurochem.*, **55**, 2015–2023.
- Kiaei, M., Kipiani, K., Chen, J., Calingasan, N.Y. and Beal, M.F. (2005) Peroxisome proliferator-activated receptor-gamma agonist extends survival in transgenic mouse model of amyotrophic lateral sclerosis. *Exp. Neurol.*, **191**, 331–336.
- Schutz, B., Reimann, J., Dumitrescu-Ozimek, L., Kappes-Horn, K., Landreth, G.E., Schurmann, B., Zimmer, A. and Heneka, M.T. (2005) The oral antidiabetic pioglitazone protects from neurodegeneration and amyotrophic lateral sclerosis-like symptoms in superoxide dismutase-G93A transgenic mice. *J. Neurosci.*, **25**, 7805–7812.
- Dumont, M., Stack, C., Elipenahli, C., Jainuddin, S., Gerges, M., Starkova, N., Calingasan, N.Y., Yang, L., Tampellini, D., Starkov, A.A. et al. (2012) Bezafibrate administration improves behavioral deficits and tau pathology in P301S mice. *Hum. Mol. Genet.*, **21**, 5091–5105.
- Johri, A., Calingasan, N.Y., Hennessey, T.M., Sharma, A., Yang, L., Wille, E., Chandra, A. and Beal, M.F. (2012) Pharmacologic activation of mitochondrial biogenesis exerts widespread beneficial effects in a transgenic mouse model of Huntington's disease. *Hum. Mol. Genet.*, **21**, 1124–1137.
- Xu, J., Racke, M.K. and Drew, P.D. (2007) Peroxisome proliferator-activated receptor-alpha agonist fenofibrate regulates IL-family cytokine expression in the CNS: relevance to multiple sclerosis. *J. Neurochem.*, **103**, 1801–1810.
- Kreisler, A., Gele, P., Wiart, J.F., Lhermitte, M., Destee, A. and Bordet, R. (2007) Lipid-lowering drugs in the MPTP mouse model of Parkinson's disease: fenofibrate has a neuroprotective effect, whereas bezafibrate and HMG-CoA reductase inhibitors do not. *Brain Res.*, **1135**, 77–84.
- Purdy, C.W., Straus, D.C., Chirase, N., Ayers, J.R. and Hoover, M.D. (2003) Effects of aerosolized dust in goats on lung clearance of *Pasteurella* and *Mannheimia* species. *Curr. Microbiol.*, **46**, 174–179.
- Rosen, D.R. (1993) Mutations in Cu/Zn superoxide dismutase gene are associated with familial amyotrophic lateral sclerosis. *Nature*, **364**, 362.

28. Johnson, J.O., Mandrioli, J., Benatar, M., Abramzon, Y., Van Deerlin, V.M., Trojanowski, J.Q., Gibbs, J.R., Brunetti, M., Gronka, S., Wu, J. et al. (2010) Exome sequencing reveals VCP mutations as a cause of familial ALS. *Neuron*, **68**, 857–864.
29. Yang, Y., Hentati, A., Deng, H.X., Dabbagh, O., Sasaki, T., Hirano, M., Hung, W.Y., Ouahchi, K., Yan, J., Azim, A.C. et al. (2001) The gene encoding ALSIN, a protein with three guanine-nucleotide exchange factor domains, is mutated in a form of recessive amyotrophic lateral sclerosis. *Nat. Genet.*, **29**, 160–165.
30. Lai, S.L., Abramzon, Y., Schymick, J.C., Stephan, D.A., Dunckley, T., Dillman, A., Cookson, M., Calvo, A., Battistini, S., Gianini, F. et al. (2011) FUS mutations in sporadic amyotrophic lateral sclerosis. *Neurobiol. Aging*, **32**, 550 e551–554.
31. Kabashi, E., Valdmanis, P.N., Dion, P., Spiegelman, D., McConkey, B.J., Vande Velde, C., Bouchard, J.P., Lacomblez, L., Pochigava, K., Salachas, F. et al. (2008) TARDBP mutations in individuals with sporadic and familial amyotrophic lateral sclerosis. *Nat. Genet.*, **40**, 572–574.
32. Daoud, H., Valdmanis, P.N., Kabashi, E., Dion, P., Dupre, N., Camu, W., Meininger, V. and Rouleau, G.A. (2009) Contribution of TARDBP mutations to sporadic amyotrophic lateral sclerosis. *J. Med. Genet.*, **46**, 112–114.
33. DeJesus-Hernandez, M., Mackenzie, I.R., Boeve, B.F., Boxer, A.L., Baker, M., Rutherford, N.J., Nicholson, A.M., Finch, N.A., Flynn, H., Adamson, J. et al. (2011) Expanded GGGGCC hexanucleotide repeat in noncoding region of C9ORF72 causes chromosome 9p-linked FTD and ALS. *Neuron*, **72**, 245–256.
34. Renton, A.E., Majounie, E., Waite, A., Simon-Sanchez, J., Rollinson, S., Gibbs, J.R., Schymick, J.C., Laaksovirta, H., van Swieten, J.C., Myllykangas, L. et al. (2011) A hexanucleotide repeat expansion in C9ORF72 is the cause of chromosome 9p21-linked ALS-FTD. *Neuron*, **72**, 257–268.
35. Al-Saif, A., Al-Mohanna, F. and Bohlega, S. (2011) A mutation in sigma-1 receptor causes juvenile amyotrophic lateral sclerosis. *Ann. Neurol.*, **70**, 913–919.
36. Maruyama, H., Morino, H., Ito, H., Izumi, Y., Kato, H., Watanabe, Y., Kinoshita, Y., Kamada, M., Nodera, H., Suzuki, H. et al. (2010) Mutations of optineurin in amyotrophic lateral sclerosis. *Nature*, **465**, 223–226.
37. Iida, A., Hosono, N., Sano, M., Kamei, T., Oshima, S., Tokuda, T., Nakajima, M., Kubo, M., Nakamura, Y. and Ikegawa, S. (2012) Novel deletion mutations of OPTN in amyotrophic lateral sclerosis in Japanese. *Neurobiol. Aging*, **33**, 1843 e1819–1824.
38. Deng, H.X., Chen, W., Hong, S.T., Boycott, K.M., Gorrie, G.H., Siddique, N., Yang, Y., Fecto, F., Shi, Y., Zhai, H. et al. (2011) Mutations in UBQLN2 cause dominant X-linked juvenile and adult-onset ALS and ALS/dementia. *Nature*, **477**, 211–215.
39. Wu, C.H., Fallini, C., Ticozzi, N., Keagle, P.J., Sapp, P.C., Piotrowska, K., Lowe, P., Koppers, M., McKenna-Yasek, D., Baron, D.M. et al. (2012) Mutations in the profilin 1 gene cause familial amyotrophic lateral sclerosis. *Nature*, **488**, 499–503.
40. Smith, B.N., Ticozzi, N., Fallini, C., Gkazi, A.S., Topp, S., Kenna, K.P., Scotter, E.L., Kost, J., Keagle, P., Miller, J.W. et al. (2014) Exome-wide rare variant analysis identifies TUBA4A mutations associated with familial ALS. *Neuron*, **84**, 324–331.
41. Cirulli, E.T., Lasseigne, B.N., Petrovski, S., Sapp, P.C., Dion, P.A., Leblond, C.S., Couthouis, J., Lu, Y.F., Wang, Q., Krueger, B.J. et al. (2015) Exome sequencing in amyotrophic lateral sclerosis identifies risk genes and pathways. *Science*, **347**, 1436–3941.
42. Wong, Y.C. and Holzbaur, E.L.F. (2014) Optineurin is an autophagy receptor for damaged mitochondria in Parkin-mediated mitophagy that is disrupted by an ALS-linked mutation. *Proc. Natl Acad. Sci. USA*, **111**, E4439–E4448.
43. Regan, M.R., Huang, Y.H., Kim, Y.S., Dykes-Hoberg, M.I., Jin, L., Watkins, A.M., Bergles, D.E. and Rothstein, J.D. (2007) Variations in promoter activity reveal a differential expression and physiology of glutamate transporters by glia in the developing and mature CNS. *J. Neurosci.*, **27**, 6607–6619.
44. Reijo, R., Lee, T.Y., Salo, P., Alagappan, R., Brown, L.G., Rosenberg, M., Rozen, S., Jaffe, T., Straus, D., Hovatta, O. et al. (1995) Diverse spermatogenic defects in humans caused by Y chromosome deletions encompassing a novel RNA-binding protein gene. *Nat. Genet.*, **10**, 383–393.
45. DeLoach, A., Cozart, M., Kiaei, A. and Kiaei, M. (2015) A retrospective review of the progress in amyotrophic lateral sclerosis drug discovery over the last decade and a look at the latest strategies. *Expert. Opin. Drug. Discov.*, **10**, 1099–118.
46. Da Costa, M.M., Allen, C.E., Higginbottom, A., Ramesh, T., Shaw, P.J. and McDermott, C.J. (2014) A new zebrafish model produced by TILLING of SOD1-related amyotrophic lateral sclerosis replicates key features of the disease and represents a tool for in vivo therapeutic screening. *Dis. Model. Mech.*, **7**, 73–81.
47. Ramesh, T.M., Shaw, P.J. and McDermid, J. (2014) Azebrafish model exemplifies the long preclinical period of motor neuron disease. *J. Neurol. Neurosurg. Psychiatry*, **85**, 1288–1289.
48. Son, E.Y., Ichida, J.K., Wainger, B.J., Toma, J.S., Rafuse, V.F., Woolf, C.J. and Eggan, K. (2011) Conversion of mouse and human fibroblasts into functional spinal motor neurons. *Cell Stem Cell*, **9**, 205–218.
49. Eschbach, J., Schwalenstocker, B., Soyak, S.M., Bayer, H., Wiesner, D., Akimoto, C., Nilsson, A.C., Birve, A., Meyer, T., Dupuis, L. et al. (2013) PGC-1alpha is a male-specific disease modifier of human and experimental amyotrophic lateral sclerosis. *Hum. Mol. Genet.*, **22**, 3477–3484.
50. Thau, N., Knippenberg, S., Korner, S., Rath, K.J., Dengler, R. and Petri, S. (2012) Decreased mRNA expression of PGC-1alpha and PGC-1alpha-regulated factors in the SOD1G93A ALS mouse model and in human sporadic ALS. *J. Neuropathol. Exp. Neurol.*, **71**, 1064–1074.
51. Damiano, M., Starkov, A.A., Petri, S., Kipiani, K., Kiaei, M., Mattiuzzi, M., Flint Beal, M. and Manfredi, G. (2006) Neural mitochondrial Ca²⁺ capacity impairment precedes the onset of motor symptoms in G93A Cu/Zn-superoxide dismutase mutant mice. *J. Neurochem.*, **96**, 1349–1361.
52. Magrane, J., Sahawneh, M.A., Przedborski, S., Estevez, A.G. and Manfredi, G. (2012) Mitochondrial dynamics and bioenergetic dysfunction is associated with synaptic alterations in mutant SOD1 motor neurons. *J. Neurosci.*, **32**, 229–242.
53. Glass, C.K. and Ogawa, S. (2006) Combinatorial roles of nuclear receptors in inflammation and immunity. *Nat. Rev. Immunol.*, **6**, 44–55.
54. Haskew-Layton, R.E., Payappilly, J.B., Xu, H., Bennett, S.A. and Ratan, R.R. (2013) 15-Deoxy-Delta12,14-prostaglandin J2 (15d-PGJ2) protects neurons from oxidative death via an Nrf2 astrocyte-specific mechanism independent of PPARgamma. *J. Neurochem.*, **124**, 536–547.
55. Milligan, C.E., Levitt, P. and Cunningham, T.J. (1991) Brain macrophages and microglia respond differently to lesions of the developing and adult visual system. *J. Comp. Neurol.*, **314**, 136–146.
56. Milligan, C.E., Cunningham, T.J. and Levitt, P. (1991) Differential immunochemical markers reveal the normal distribution of brain macrophages and microglia in the developing rat brain. *J. Comp. Neurol.*, **314**, 125–135.

57. Hondares, E., Pineda-Torra, I., Iglesias, R., Staels, B., Villarroya, F. and Giral, M. (2007) PPARdelta, but not PPARalpha, activates PGC-1alpha gene transcription in muscle. *Biochem. Biophys. Res. Commun.*, **354**, 1021–1027.
58. Bastin, J., Aubey, F., Rotig, A., Munnich, A. and Djouadi, F. (2008) Activation of peroxisome proliferator-activated receptor pathway stimulates the mitochondrial respiratory chain and can correct deficiencies in patients' cells lacking its components. *J. Clin. Endocrinol. Metab.*, **93**, 1433–1441.
59. Fukunaga, K., Shinoda, Y. and Tagashira, H. (2015) The role of SIGMAR1 gene mutation and mitochondrial dysfunction in amyotrophic lateral sclerosis. *J. Pharmacol. Sci.*, **127**, 36–41.
60. Besson, V.C., Chen, X.R., Plotkine, M. and Marchand-Verrecchia, C. (2005) Fenofibrate, a peroxisome proliferator-activated receptor alpha agonist, exerts neuroprotective effects in traumatic brain injury. *Neurosci. Lett.*, **388**, 7–12.
61. Ouk, T., Laprais, M., Bastide, M., Mostafa, K., Gautier, S. and Bordet, R. (2009) Withdrawal of fenofibrate treatment partially abrogates preventive neuroprotection in stroke via loss of vascular protection. *Vascul. Pharmacol.*, **51**, 323–330.
62. Sehgal, N., Kumawat, K.L., Basu, A. and Ravindranath, V. (2012) Fenofibrate reduces mortality and precludes neurological deficits in survivors in murine model of Japanese encephalitis viral infection. *PLoS One*, **7**, e35427.
63. Tenenbaum, A., Motro, M., Fisman, E.Z., Tanne, D., Boyko, V. and Behar, S. (2005) Bezafibrate for the secondary prevention of myocardial infarction in patients with metabolic syndrome. *Arch. Intern. Med.*, **165**, 1154–1160.
64. Wenz, T., Williams, S.L., Bacman, S.R. and Moraes, C.T. (2010) Emerging therapeutic approaches to mitochondrial diseases. *Dev. Disabil. Res. Rev.*, **16**, 219–229.
65. Da Cruz, S., Parone, P.A., Lopes, V.S., Lillo, C., McAlonis-Downes, M., Lee, S.K., Vetto, A.P., Petrosyan, S., Marsala, M., Murphy, A.N. et al. (2012) Elevated PGC-1alpha activity sustains mitochondrial biogenesis and muscle function without extending survival in a mouse model of inherited ALS. *Cell. Metab.*, **15**, 778–786.
66. Jeong, S., Han, M., Lee, H., Kim, M., Kim, J., Nicol, C.J., Kim, B.H., Choi, J.H., Nam, K.H., Oh, G.T. et al. (2004) Effects of fenofibrate on high-fat diet-induced body weight gain and adiposity in female C57BL/6J mice. *Metabolism*, **53**, 1284–1289.
67. Dupuis, L., Corcia, P., Fergani, A., Gonzalez De Aguilar, J.L., Bonnefont-Rousselot, D., Bittar, R., Seilhean, D., Hauw, J.J., Lacomblez, L., Loeffler, J.P. et al. (2008) Dyslipidemia is a protective factor in amyotrophic lateral sclerosis. *Neurology*, **70**, 1004–1009.
68. Wills, A.M., Hubbard, J., Macklin, E.A., Glass, J., Tandan, R., Simpson, E.P., Brooks, B., Gelinas, D., Mitsumoto, H., Mozaffar, T. et al. (2014) Hypercaloric enteral nutrition in patients with amyotrophic lateral sclerosis: a randomised, double-blind, placebo-controlled phase 2 trial. *Lancet*, **383**, 2065–2072.
69. Gurney, M.E., Pu, H., Chiu, A.Y., Dal Canto, M.C., Polchow, C.Y., Alexander, D.D., Caliendo, J., Hentati, A., Kwon, Y.W., Deng, H.X. et al. (1994) Motor neuron degeneration in mice that express a human Cu,Zn superoxide dismutase mutation. *Science*, **264**, 1772–1775.
70. Kiaei, M., Kipiani, K., Petri, S., Chen, J., Calingasan, N.Y. and Beal, M.F. (2005) Celastrol blocks neuronal cell death and extends life in transgenic mouse model of amyotrophic lateral sclerosis. *Neurodegener. Dis.*, **2**, 246–254.
71. Kiaei, M., Petri, S., Kipiani, K., Gardian, G., Choi, D.K., Chen, J., Calingasan, N.Y., Schafer, P., Muller, G.W., Stewart, C. et al. (2006) Thalidomide and lenalidomide extend survival in a transgenic mouse model of amyotrophic lateral sclerosis. *J. Neurosci.*, **26**, 2467–2473.
72. Livak, K.J. and Schmittgen, T.D. (2001) Analysis of relative gene expression data using real-time quantitative PCR and the 2^{-Delta Delta C(T)} method. *Methods*, **25**, 402–408.
73. Kaidery, N.A., Banerjee, R., Yang, L., Smirnova, N.A., Hushpalian, D.M., Liby, K.T., Williams, C.R., Yamamoto, M., Kensler, T.W., Ratan, R.R. et al. (2013) Targeting Nrf2-mediated gene transcription by extremely potent synthetic triterpenoids attenuate dopaminergic neurotoxicity in the MPTP mouse model of Parkinson's disease. *Antioxid. Redox Signal.*, **18**, 139–157.
74. Kulkarni, R.K. and Straus, D.S. (1983) Insulin-mediated phosphorylation of ribosomal protein S6 in mouse melanoma cells and melanoma x fibroblast hybrid cells in relation to cell proliferation. *Biochim. Biophys. Acta.*, **762**, 542–551.